International Conference
**Nuclear Energy in Central Europe 2001**
**Hoteli Bernardin, Portorož, Slovenia, September 10-13, 2001**
www: http://www.drustvo-js.si/port2001/ e-mail: PORT2001@ijs.si
tel.:+ 386 1 588 5247, + 386 1 588 5311 fax:+ 386 1 561 2335
Nuclear Society of Slovenia, PORT2001, Jamova 39, SI-1000 Ljubljana, Slovenia

# DEVELOPMENT OF AN INTEGRAL COMPUTER CODE FOR SIMULATION OF HEAT EXCHANGERS

**Andrej Horvat**
"Jožef Stefan" Institute, Reactor Engineering Division
Jamova 39, SI-1000 Ljubljana, Slovenia
andrej.horvat@ijs.si

**Ivan Catton**
Morrin-Martinelli-Gier Memorial Heat Transfer Laboratory
Department of Mechanical and Aerospace Engineering
School of Engineering and Applied science
University of California, Los Angeles

## ABSTRACT

Heat exchangers are one of the basic installations in power and process industries. The present guidelines provide an ad-hoc solution to certain design problems. A unified approach based on simultaneous modeling of thermal-hydraulics and structural behavior does not exist. The present paper describes the development of integral numerical code for simulation of heat exchangers. The code is based on Volume Averaging Technique (VAT) for porous media flow modeling. The calculated values of the whole-section drag and heat transfer coefficients show an excellent agreement with already published values. The matching results prove the correctness of the selected approach and verify the developed numerical code used for this calculation.

## 1 INTRODUCTION

Heat exchangers are one of the basic installations in power and process industries. This is especially true for PWRs, where the steam generator is the heat transfer interface between the primary and the secondary circuit. Despite their crucial role, there is still a great deal of empiricism involved in the design procedure of heat exchangers. Although present guidelines provide an ad-hoc solution to the design problems, a unified approach based on simultaneous modeling of thermal-hydraulics and structural behavior does not exist. As a result, designs are overly constrained with a resulting economic penalty. Therefore, the optimization of a heat exchanger design can bring significant cost reduction to industry.

The present paper is a part of a broader effort which is ongoing in the Morrin-Martinelli-Gier Memorial Heat Transfer Laboratory at University of California, Los Angeles to develop a scientific procedure for optimization of heat exchanger geometry. As a part of this program an integral numerical code for modeling of heat exchangers was constructed. The numerical code is based on Volume Averaging Technique (VAT) for a porous media flow, which was presented by Whiteker [1] and further developed by Travkin and Catton [2,

3]. Treating the heat exchanger structure as a uniform porous media makes the numerical code fast running and suitable for the surface optimization calculations.

## 2 GEOMETRICAL CONSIDERATIONS

The geometry of the simulated test section is presented on fig. 1. It is the same as the experimental test section in the Morrin-Martinelli-Gier Memorial Heat Transfer Laboratory, where a fluid behavior during induced finite amplitude tube vibrations has been studied. In this case water has been taken as a coolant and stainless steel as a tube material. The tubes had staggered arrangement with a diameter $d$ =1" (0.0254m). The pitch to diameter ratio was set to $p/d$ = 1.4.

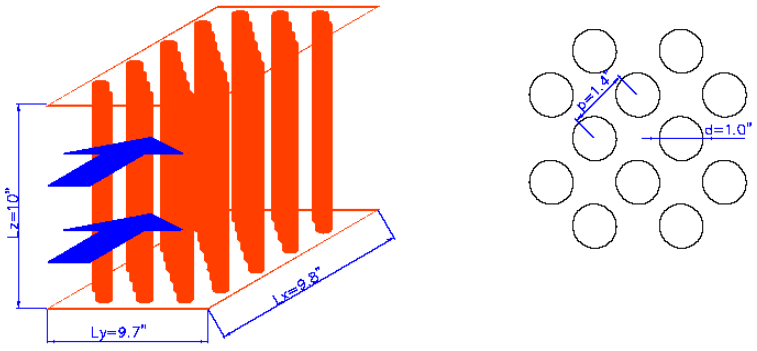


(a) (b)

**Figure 1:** Simulated section of a heat exchanger (a); tube arrangement (b)

The inlet water temperature was 293K (20°C). The bottom and top boundaries as well as the internal structure were taken as isothermal with the temperature set to 296K (23°C). The sidewalls were considered to be adiabatic. For velocity, no-slip boundary conditions were assigned on the bottom and top walls and slip boundary conditions on the sidewalls.

The pressure drop across the test section was adjusted so that flow regimes at Reynolds numbers from $Re$ =10 to 1000 could be examined.

## 3 GOVERNING EQUATIONS

For the described heat transfer problem, the basic transport equations for fluid flow (eq. 1-3) are:

$$\partial_i v_i = 0 \tag{1}$$

$$\rho_f v_j \partial_j v_i = -\partial_i p + \mu_f \partial_j \partial_j v_i \tag{2}$$

$$\rho_f c_f v_j \partial_j T_f = \lambda_f \partial_j \partial_j T_f \tag{3}$$

In order to obtain transport equations for phase averaged variables, volumetric averaging, see Travkin and Catton [3] for details, was applied to the above equations. In the averaged eqns. (4-6), the phase averaged variables are denoted with ˜ and the phase index ($f$ or $s$). Thus, the fluid transport eqns. (1-3) are transformed to:

$$\partial_i \tilde{v}_i = 0 \tag{4}$$

$$\alpha_f \rho_f \widetilde{v}_j \partial_j \widetilde{v}_i = -\alpha_f \partial_i \widetilde{p} + \alpha_f \mu_f \partial_j \partial_j \widetilde{v}_i - \frac{1}{\Omega}\int_{\partial\Omega} p\, d\vec{s} + \frac{1}{\Omega}\int_{\partial\Omega} \mu_f \partial_j v_i\, d\vec{s} \tag{5}$$

$$\alpha_f \rho_f c_f \widetilde{v}_j \partial_j \widetilde{T}_f = \alpha_f \lambda_f \partial_j \partial_j \widetilde{T}_f + \frac{1}{\Omega}\int_{\partial\Omega} \lambda_f \partial_j T_f d\vec{s} \tag{6}$$

The spatial scale of the phase averaged values (4-6) is much larger than the scale of the local values (1-3) as a result of the volumetric averaging. This can enable much faster calculation of phase averaged values, but only if the integrals on the right-hand-side of eqns. (4-6) are solved efficiently.

The integrals in eqns. (4-6) are a consequence of the volumetric averaging. They capture momentum (5) and energy transport (6) on the fluid-solid interface. Similar to turbulent flow, separate models in the form of closure relations are needed. In the present case, the integrals in eqns. (4-6) are replaced with drag (8) and heat transfer (9) relations. The resulting eqns. are

$$\partial_i \widetilde{v}_i = 0 \tag{7}$$

$$\alpha_f \rho_f \widetilde{v}_j \partial_j \widetilde{v}_i = -\alpha_f \partial_i \widetilde{p} + \alpha_f \mu_f \partial_j \partial_j \widetilde{v}_i - \frac{1}{2} C_d \rho_f \widetilde{v}_i^2 dx_i^{-1} \tag{8}$$

$$\alpha_f \rho_f c_f v_j \partial_j \widetilde{T}_f = \alpha_f \lambda_f \partial_j \partial_j \widetilde{T}_f - hS_w \left(\widetilde{T}_f - \widetilde{T}_s\right) \tag{9}$$

The closure relations in eqns. (7-9) simulate system local behavior with the averaged values. In order to succeed in this contradictory task, additional information in form of drag (8) and heat transfer (9) coefficients have to be added to the transport equations (7-9). For these coefficients, reliable experimental data were found in Žukauskas and Ulinskas [4].

To further simplify the simulated system, the fluid flow was taken as unidirectional with a constant pressure drop. As a consequence, the velocity changes only transverse to the flow direction. This means that the streamwise pressure gradient across the entire simulation domain is balanced with shear stresses in the transverse ($z$) direction:

$$-\alpha_f \mu_f \partial_z \partial_z \widetilde{v}_x L_x + \frac{1}{2} C_d \rho_f \widetilde{v}_x^2 = \alpha_f \Delta\widetilde{p} \tag{10}$$

where $\Delta p$ is positive.

Due to the thermal boundary conditions, the temperature field is two-dimensional, changing its values in vertical ($z$) and streamwise ($x$) directions. As shown by the energy eqn. (11), thermal convection in the streamwise direction is balanced by diffusion due to a vertical temperature profile as well as with heat transferred from isothermal tubes:

$$\alpha_f \rho_f c_f \widetilde{v}_x \partial_x \widetilde{T}_f = \alpha_f \lambda_f \partial_z \partial_z \widetilde{T}_f - hS_w \left(\widetilde{T}_f - \widetilde{T}_s\right) \tag{11}$$

## 4 NUMERICAL METHODS

Due to the boundary conditions, velocity $\widetilde{v}_x$ can be described as a one-dimensional and temperature as a two-dimensional scalar field. Nevertheless, the constructed numerical code

calculates the velocity as a two-dimensional and temperature as a three-dimensional scalar field. These numerical code extensions and the additional computational effort were invested in order to be able to treat three-dimensional thermal problems in the future.

The momentum equation (10) was discretized using a central-symmetric scheme that resulted in the five diagonal matrix system:

$$
\begin{aligned}
&-\frac{\Delta_y}{\Delta_z^-}\left\{\tilde{v}_x^{\,new}\right\}_{k-1,j}-\frac{\Delta_z}{\Delta_y^-}\left\{\tilde{v}_x^{\,new}\right\}_{k,j-1}\\
&+\left(\frac{\Delta_y}{\Delta_z^-}+\frac{\Delta_z}{\Delta_y^-}+\frac{\Delta_z}{\Delta_y^+}+\frac{\Delta_y}{\Delta_z^+}+\frac{C_d}{2\alpha_f \nu_f L_x}\Delta_y\Delta_z\left\{\tilde{v}_x^{\,old}\right\}_{k,j}\right)\left\{\tilde{v}_x^{\,new}\right\}_{k,j}\\
&-\frac{\Delta_z}{\Delta_y^+}\left\{\tilde{v}_x^{\,new}\right\}_{k,j+1}-\frac{\Delta_y}{\Delta_z^+}\left\{\tilde{v}_x^{\,new}\right\}_{k+1,j}=\frac{\Delta\tilde{p}}{\rho_f \nu_f L_x}\Delta_y\Delta_z
\end{aligned}
\tag{12}
$$

Although the matrix (eq. 12) is symmetrical, it has non-constant terms on the central diagonal due to non-linearity of the drag force term.

In the energy equation (11), the convection term was discretized using an upwind scheme, whereas for the diffusion term, a central-symmetric scheme was applied:

$$
\begin{aligned}
&-\left(\frac{\rho_f c_f}{\lambda_f}\Delta_y\Delta_z\left\{\tilde{v}_x\right\}_{k,j,i-1}+\frac{\Delta_y\Delta_z}{\Delta_x^-}\right)\left\{\tilde{T}_f^{\,new}\right\}_{k,j,i-1}-\frac{\Delta_x\Delta_y}{\Delta_z^-}\left\{\tilde{T}_f^{\,new}\right\}_{k-1,j,i}-\frac{\Delta_x\Delta_z}{\Delta_y^-}\left\{\tilde{T}_f^{\,new}\right\}_{k,j-1,i}\\
&+\left(\begin{array}{l}\dfrac{\Delta_y\Delta_z}{\Delta_x^-}+\dfrac{\Delta_x\Delta_y}{\Delta_z^-}+\dfrac{\Delta_x\Delta_z}{\Delta_y^-}+\dfrac{\Delta_x\Delta_z}{\Delta_y^+}+\dfrac{\Delta_x\Delta_y}{\Delta_z^+}+\dfrac{\Delta_y\Delta_z}{\Delta_x^+}+\\ \dfrac{\rho_f c_f}{\lambda_f}\Delta_y\Delta_z\left\{\tilde{v}_x\right\}_{k,j,i}+\dfrac{hS_w}{\alpha_f\lambda_f}\Delta_x\Delta_y\Delta_z\end{array}\right)\left\{\tilde{T}_f^{\,new}\right\}_{k,j,i}\\
&-\frac{\Delta_x\Delta_z}{\Delta_y^+}\left\{\tilde{T}_f^{\,new}\right\}_{k,j+1,i}-\frac{\Delta_x\Delta_y}{\Delta_z^+}\left\{\tilde{T}_f^{\,new}\right\}_{k+1,j,i}-\frac{\Delta_y\Delta_z}{\Delta_x^+}\left\{\tilde{T}_f^{\,new}\right\}_{k,j,i+1}=\frac{hS_w\tilde{T}_s}{\alpha_f\lambda_f}\Delta_x\Delta_y\Delta_z
\end{aligned}
\tag{13}
$$

In this case the resulting seven diagonal matrix system is not symmetrical due to the upwind discretization, nor does it have constant terms due to the locally changing heat transfer coefficient $h$.

In order to invert the matrix systems (12 & 13) efficiently, a preconditioned conjugate gradient method, described by Ferziger and Perić [5], was adopted for this specific problem.

## 5 RESULTS AND DISCUSSION

Simulations were performed for Reynolds numbers ranging from $Re$ = 10 to $Re$ = 1000 at a pitch-to-diameter ratio of $p/d$ = 1.4. The whole-section drag coefficient $C_d$, which is locally defined by

$$\frac{1}{2}C_d\rho_f\tilde{v}_x^2=\alpha_f\Delta\tilde{p}_d \tag{14}$$

is plotted on a log-log diagram, fig. 2, as a function of Reynolds number $Re$. The experimental as well as the computational results of Žukauskas and Ulinskas [4], Launder and Massey [6], Bergalin et. al [7] and LeFeuvre [8] are added for comparison.

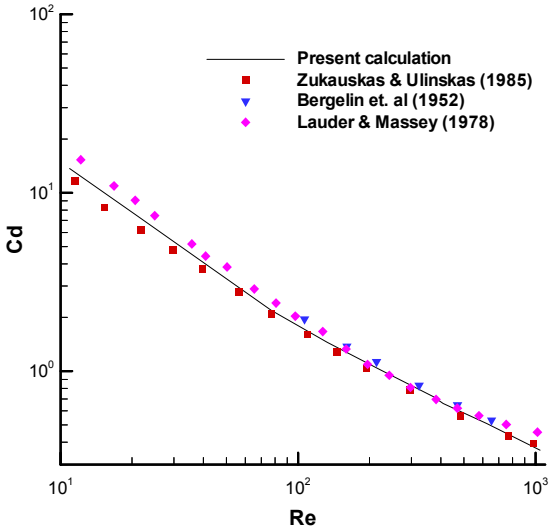


**Figure 2:** Reynolds number *Re* versus whole-section drag coefficient $C_d$.

Although the computed results are still preliminary, they show excellent agreement with the experimental results of Bergelin et al. [7] and Žukauskas and Ulinskas [4] as well as with numerical results of Launder and Massey [6] for similar pitch-to-diameter ratios.

Žukauskas [9] defined the coefficient $K_f$ to account for temperature dependence in experimental data :

$$K_f = Nu_f \, Pr_f^{-0.36} \left( \frac{Pr_f}{Pr_w} \right)^{-0.25} \tag{15}$$

It is used here to compare our heat transfer coefficient calculations with available data. In this case, subscript $w$ denotes wall temperature and subscript $f$ fluid average temperature, calculated as a mean value between inflow and wall temperature.

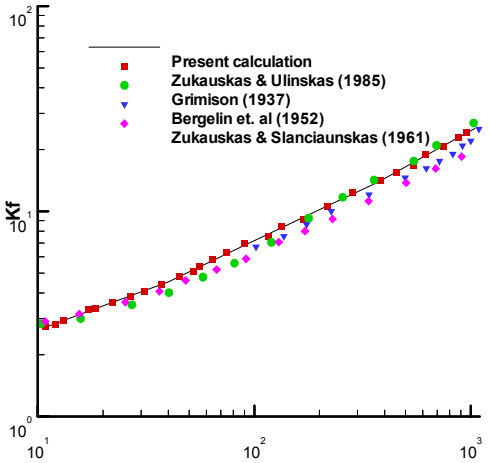


**Figure 3:** Reynolds number *Re* versus coefficient $K_f$.

Fig. 3 presents the calculated values of the coefficient $K_f$ together with values obtained from experimental and numerical results of Žukauskas and Ulinskas [4], Bergelin et. al [7],

Grimison [10] and Žukauskas and Šlančiaunskas [11]. The calculated values of the coefficient $K_f$ are in close agreement with the previously published data.

Three different linear regions can be identified in the $Re$-$K_f$ relationship shown in fig.3. The first region is for Reynolds numbers $Re<50$, the second for Reynolds numbers $50<Re<615$ and the third for Reynolds numbers $615<Re$. As is evident from fig. 3, the value of $K_f$ increases faster as Reynolds number increases.

Table 1 summarizes values of Nusselt number $Nu_f$ and thermal power $Q$ as functions of Reynolds number. In contrast to the Nusselt number $Nu_f$, which is directly determined by the selection of experimental values of local heat transfer coefficient $h$, the values of thermal power $Q$ must be calculated from the fluid inlet and outlet temperatures:

$$Q = \alpha_f c_f \rho_f \tilde{v}_x \left(\tilde{T}_{out} - \tilde{T}_{in}\right)_f \qquad (16)$$

**Table 1:** Nusselt number and thermal power as a function of Reynolds number

| ***Re*** | ***Nu*** | ***Q* [W]** |
|---|---|---|
| 10.93 | 5.5 | 147.2 |
| 20.95 | 7.1 | 257.6 |
| 40.17 | 9.2 | 427.0 |
| 77.09 | 13 | 699.7 |
| 132.8 | 17 | 1026 |
| 222.4 | 22 | 1445 |
| 372.6 | 28 | 2004 |
| 624.4 | 38 | 2843 |
| 1047 | 52 | 3990 |

Figure 4 presents the fluid temperature fields. To clearly show how the temperature field changes with the flow regime, only the cases at the lowest and highest Reynolds number are presented.

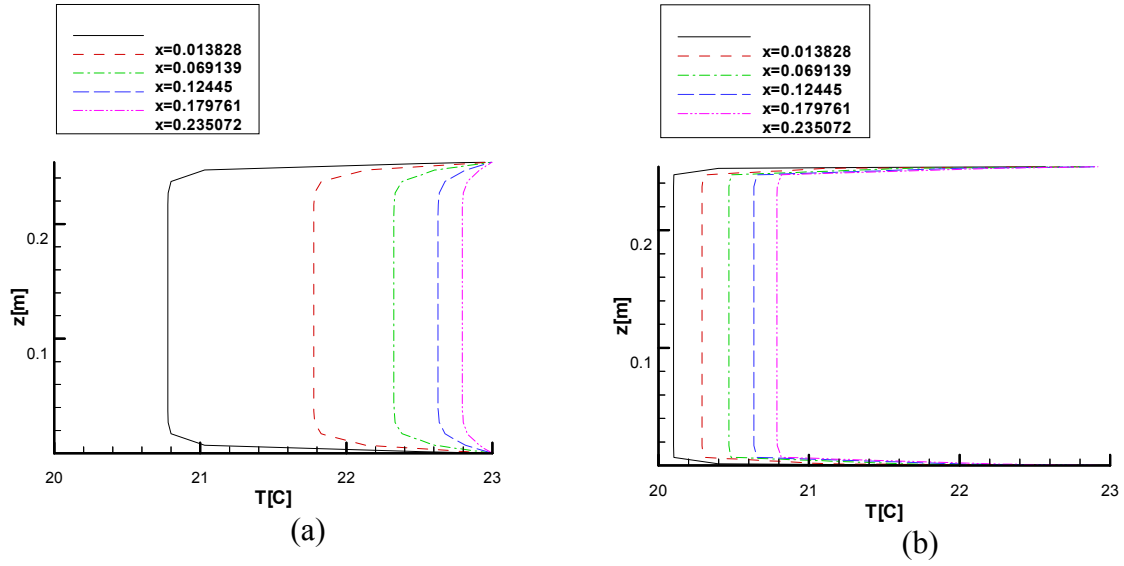


**Figure 4:** Temperature profiles at Reynolds number $Re$ = 10.93 (a) and $Re$ = 1046.7 (b)

At a Reynolds number of *Re* ~10 (fig. 4a), the isothermal tubes immersed into a cross-flow with domain walls at the tube temperature manage to heat the fluid almost to the heating surface temperature; the fluid temperature in the core of the flow raises from 20.0 $^{o}$C to 20.8 $^{o}$C after 1.38 cm and reaches 22 $^{o}$C at the section end. The vertical thermal diffusion from the bottom and top walls is also strong forming a thick thermal boundary layer.

At a Reynolds number of *Re* ~1000 (fig. 4b), the water leaves the simulated section with a temperature of 20.8 $^{o}$C. This indicates that with the imposed increase in Reynolds number the increase in heat transfer from the structure to the flow is smaller than the increased heat carrying capability. Namely, after passing the simulated section, the water still has a potential for heat removal. Further, the thermal boundary layer next to the walls becomes much thinner than in the former case, due to a dominating convection in a streamwise direction.

## 6 CONCLUSIONS

The present paper describes the construction of a fast running numerical procedure for heat exchanger calculations. The heat exchanger internal structure, in form of isothermal tubes, was treated as a homogenous porous media. The local values of drag and heat transfer coefficients that were needed to close the transport equations were taken from Žukauskas and Ulinskas [4]. The resulting partial differential equations were discretized using the conservation properties of the finite volume method. The resulting system of semilinear equations was then solved with a preconditioned conjugate gradient method. As a benchmark configuration, an experimental test section that has been used in the Morrin-Martinelli-Gier Memorial Heat Transfer Laboratory for steam-tube vibration studies was selected.

The calculated values of the whole-section drag and the heat transfer coefficients show excellent agreement with published data. The matching results demonstrate that the selected approach is appropriate for heat exchanger calculations and verify that the numerical code developed for this calculation yields accurate results.

In the paper the fluid temperature fields are also presented. The fluid isotherms show that increasing Reynolds number *Re* does not increase heat transfer as fast as the heat carrying capacity of the fluid. As a consequence the fluid leaves the heat exchanger capable of more heat removal.

## ACKNOWLEDGEMENTS

The first author wishes to thank K. Hu and Prof. I. Catton for all the helpful explanations and valuable comments. The first author's financial support by the Kerze-Cheyovich scholarship is also gratefully acknowledged.

## NOMENCLATURE

| | |
|---|---|
| $c$ | specific heat |
| $C_d$ | drag coefficient |
| $d$ | diameter |
| $h$ | heat transfer coefficient |
| $L$ | length of simulation domain |
| $K_f$ | heat transfer coefficient (Žukauskas [4]) |
| $Nu$ | Nusselt number |
| $p$ | pressure, pitch |
| $Q$ | thermal power |
| $Pr$ | Prandtl number |
| $Re$ | Reynolds number |
| $s$ | surface |
| $S_w$ | specific interface surface |
| $v$ | velocity |
| $T$ | temperature |
| $x$ | spatial coordinate |

*Subscripts / Superscripts*

| | |
|---|---|
| $i, j, k$ | direction indices |
| $f$ | fluid phase |
| $new$ | next iteration step |
| $old$ | previous iteration step |
| $s$ | solid phase |
| $w$ | wall |
| $+$ | next grid volume |
| $-$ | previous grid volume |

*Greek letters*

| | |
|---|---|
| $\alpha$ | phase fraction |
| $\rho$ | density |
| $\Omega$ | control volume |
| $\Delta$ | finite difference |
| $\mu$ | dynamic viscosity |
| $\nu$ | kinematic viscosity |

## REFERENCES


[1] S. Whitaker, 1967, "Diffusion and Dispersion in Porous Media". *AIChE Journal*, Vol. 13, No. 3, pp. 420-427.

[2] V.S., Travkin, I., Catton, 1995, "A Two Temperature Model for Fluid Flow and Heat Transfer in a Porous Layer". *J. Fluid Engineering*, Vol. 117, pp. 181-188.

[3] V.S., Travkin, I., Catton, 1999, "Transport Phenomena in Heterogeneous Media Based on Volume Averaging Theory". *Advans. Heat Trasfer*, Vol. 34, pp. 1-143.

[4] A.A., Žukauskas, R., Ulinskas, 1985, "Efficiency Parameters for Heat Transfer in Tube Banks". *J. Heat Transfer Engineering*, Vol.5, No.1, pp. 19-25.

[5] J.H., Ferziger, Perić, M., 1996, *Computational Method for Fluid Mechanics, Chapter 5: Solution of Linear Equation Systems*. Springer Verlag, Berlin, pp. 85-127.

[6] B.E., Launder, T.H., Massey, 1978, "The Numerical Prediction of Viscous Flow and Heat Transfer in Tube Bank". *Trans. ASME J. Heat Transfer*, Vol. 100, pp. 565-571.

[7] O.P., Bergelin, G.A., Brown, H.L., Hell, S.C., Doberstein, 1952, "Heat Transfer and Fluid Friction during Flow across Banks of Tubes, IV: A Study of Transition Zone between Viscous and Turbulent Flow". *Trans. ASME*, Vol. 74, pp. 953-960.

[8] R.F., LeFeuvre, 1973, *Laminar and Turbulent Forced Convection Processes through In-Line Tube Banks*. Imperial College London, Mech. Eng. Dept., HTS/74/5.

[9] A.A., Žukauskas, 1972, "Heat Transfer from Tubes in Crossflow", *Advances in Heat Transfer*, Vol. 8, pp. 93-160.

[10] E.D., Grimison, 1937, *Trans. ASME*, Vol. 59, p. 583.

[11] A.A., Žukauskas, A.A., Šlančiaunskas, 1961, *Teploenergetika*, No.2, p. 72.